

Latent-TGF- β has a domain swapped architecture

Stephen Nishimura

stephen.nishimura@ucsf.edu

University of California, San Francisco <https://orcid.org/0000-0003-2312-4113>

Mingliang Jin

University of California San Francisco

Robert Seed

University of California San Francisco

Tiffany Shing

University of California San Francisco

Yifan Cheng



HHMI/University of California San Francisco <https://orcid.org/0000-0001-9535-0369>

Brief Communication

Keywords:

Posted Date: November 1st, 2024

DOI: <https://doi.org/10.21203/rs.3.rs-5154292/v1>

License:   This work is licensed under a Creative Commons Attribution 4.0 International License. [Read Full License](#)

Additional Declarations: Yes there is potential Competing Interest. S.L.N. is on the scientific advisory board (SAB) of Corbus Pharmaceuticals, LLC. Y.C. is on the SABs of ShuiMu BioSciences Ltd. and Pamplona Therapeutics.

Abstract

The multifunctional cytokine TGF- β is produced in a latent form (L-TGF- β) where a RGD containing homodimeric prodomain forms a “ring” encircling mature TGF- β , shielding it from its receptors. Thus L-TGF- β must be activated to function, a process driven by dynamic allostery resulting from integrin binding the L-TGF- β RGD motif. Here we provide critical evidence that defines a domain-swapped architecture of L-TGF- β , an essential component in the dynamic allostery mechanism of L-TGF- β activation.

Introduction

TGF- β is an essential multifunctional cytokine with diverse functions in morphogenesis, extracellular matrix (ECM) and immune homeostasis¹. Understanding the regulation of TGF- β function is paramount to dissect the roles of TGF- β in disease and to facilitate targeting for therapeutic benefit. For TGF- β to function, it must be exposed or released from its latent complex to engage TGF- β receptors through a process known as activation that is mainly mediated by binding to several integrins^{2,3}. Latent-TGF- β (L-TGF- β) is composed of a disulfide-linked homodimeric prodomain which contains integrin binding arm domains connected to a straitjacket domain with a lasso loop encircling the furin cleaved mature disulfide-linked homodimeric TGF- β growth factor⁴ (Fig. 1a and b). The lasso loops are flanked by the prodomain a1 and a2 helices which form the remaining key components of the straitjacket that maintain latency (Fig. 1b)⁵. During biosynthesis, N-terminal cysteines on loop preceding the a1-helices covalently link to cysteines in milieu molecules such as GARP or LTBP1 that have a binding interface stabilizing both the growth factor and the straitjacket⁶.

We have recently shown that genetically engineering a loss-of-function mutation into this furin cleavage site results in mice that survive and are rescued from the lethal early tissue inflammation seen in *tgfb1* knock-out mice. These findings demonstrate that release of TGF- β from L-TGF- β is not required for its function⁷. For TGF- β activation to occur without release, TGF- β must be sufficiently exposed to interact with its receptors. Since the lasso loops of the straitjacket cover the receptor binding domains (RBD) on the tips of mature TGF- β , these loops must be sufficiently flexible after integrin binding to allow exposure of mature TGF- β . We found that binding of integrin α v β 8 to the RGD motif on the L-TGF- β arm domains induces flexibility preferentially to the contralateral straitjacket/lasso. This process is driven by dynamic allostery via redistribution of conformational entropy from the integrin binding site across the latent ring to increase the flexibility of the lasso loop (Fig. 1a). Increased flexibility of the lasso loop exposes the contralateral growth factor RBD to TGF- β receptors on the L-TGF- β /GARP expressing cell⁷.

Defining the architecture of L-TGF- β is essential to understand how entropy is redistributed from the arm domain across the TGF- β latent ring to the contralateral lasso upon integrin α v β 8 binding. All available crystal structures of L-TGF- β assume same architecture where the straitjacket/lasso loop is on the ipsilateral RGD containing arm domain, but such architecture is assigned arbitrarily since the linker density was not resolved (Extended data Fig. 1a)^{5,6,8-10}. AlphaFold predicts both non-swapped ipsilateral and

swapped contralateral architectures (Fig. 1b). This ambiguity raises an essential question to understand the structural basis of entropy redistribution for L-TGF-b activation, is entropy redistributed from the arm domain of one subunit to the lasso of the other subunit in an ipsilateral architecture, or within the same subunit in a domain swapped contralateral architecture? Here, we provide experimental evidence to definitely assign the domain swapped contralateral architecture to L-TGF-b.

Results and discussion

In our recent study, we analyzed the cryo-EM structure of L-TGF-b1/GARP, where a weak density links the arm domain to the contralateral straitjacket domain (Extended data Fig. 1b left)⁷, contradicting the presumed ipsilateral architecture (Fig. 1b, left). However, this density is insufficiently robust to definitively define the domain architecture. Thus, the domain architecture of L-TGF-b remains ambiguous, due to the challenge of obtaining a high-resolution structure of this flexible loop region.

To define the domain architecture of L-TGF-b1, we create a system in which the architecture can be unambiguously identified without the need for a high-resolution structure. We generated two versions of a L-TGF-b1 expression plasmid (Fig. 1c), one has the intact RGD binding site and has its TGF-b1 lasso loop (lasso1) replaced by the equivalent one from L-TGF-b3 (lasso3), and the other has the intact lasso1 but contains a RGE mutation in its integrin binding motif. Both plasmids contain the R249A furin cleavage site mutation so that mature TGF-b1 remains covalently bound within the latent complex. We transfect these two plasmids in equal quantity together with GARP (Fig. 1c). The protein products, either in ipsilateral or contralateral architectures, consist of three versions of the L-TGF-b1 dimer each covalently linked with a single GARP (Fig. 1d). One dimer has a mixture of two mutant monomers, one with a RGE motif and other with a lasso3 loop. Thus, the RGD motif and lasso3 are either on the same side of the ring in ipsilateral or on opposite sides in the contralateral architecture (Fig. 1d left). The other two mutant dimers are symmetric (Fig. 1d middle and right).

We incubate these purified L-TGF-b1/GARP mutants with avb8 followed by SEC to exclude mutant L-TGF-b1 with two RGE monomers that cannot bind integrin (Fig. 1e). We then add the antibody clone 28G11 that only recognizes the lasso1 loop¹¹ to further identify the asymmetric dimer by single particle cryo-EM (Fig. 1f-i). The prediction is that 28G11 and avb8 bind this asymmetric L-TGF-b mutant on the opposite sides in the ipsilateral or the same side in the contralateral architecture (Fig. 1h). Indeed, 2D class averages and 3D reconstruction of the complex even at a modest nominal resolution of $\sim 7 \text{ \AA}$ clearly show that 28G11 only binds to the lasso on the same side as bound integrin. Docking the atomic models of L-TGF-b1/GARP and a generic Fab into this density map confirms this assignment. Together, our experimental design with a clear logic provides a concise and straightforward result demonstrating the domain swapped contralateral architecture (Fig. 1i, and Extended Data Fig. 1c). Thus, avb8 binding redistributes conformational entropy within the same monomer in the latent ring.

The domain swapped architecture of L-TGF-b has mechanistic implications beyond avb8-mediated TGF-b activation. The integrin avb6 also binds to and activates L-TGF-b but is hypothesized to involve actin-cytoskeletal force-induced deformation and release of mature TGF-b from L-TGF-b. This hypothesis was

supported by molecular dynamics simulations based on the models with an ipsilateral domain architecture⁸. These simulations applying retrograde force through the b6 cytoplasmic domain preferentially deformed the ipsilateral protomer releasing mature TGF- β ⁸. It will be interesting to see how dynamic simulations of force-induced avb6-mediated TGF- β activation are impacted by the domain-swapped architecture.

The domain swapped architecture of L-TGF- β 1 is likely to apply to other L-TGF- β isoforms since the linker region of L-TGF- β 2 and L-TGF- β 3 are of similar length as L-TGF- β 1 (Extended Data Fig. 1d). Indeed, we do observe a weak density of the connector in L-TGF- β 3/GARP⁷ consistent with the domain swapped architecture (Extended Data Fig. 1b right). Interestingly, the TGF- β 3 connector contains a cysteine that based on its location would easily form a disulfide linkage with the connector on the other monomer in the domain swapped contralateral architecture, but likely remains unpaired in the non-domain swapped ipsilateral configuration (Extended Data Fig. 1d).

Amongst other TGF- β superfamily members, the domain swapped architecture was clearly seen in the crystal structure of Activin A, and was also assigned to myostatin, although a connector density was not seen (Extended Data Fig. 1e)^{12,13}. Our work shows an approach that may help in determining the domain architecture of myostatin and other TGF- β superfamily members, which all have prodomains that non-covalently link to their growth factors¹⁴. In conclusion, definitively defining the domain architecture of L-TGF- β and its related superfamily members is critical to understand the mechanism of latency and activation.

Method

Recombinant protein expression

L-TGF- β 1_RGD_Lasso3 (where the A31-L44 in lasso1 loop was swapped with T31-V42 from the L-TGF- β 3 lasso3 loop) has been previously described⁷. To produce L-TGF- β 1 RGD_lasso3/L-TGF- β 1 RGE_lasso1/GARP, Expi293 cells were transiently transfected with equal amounts of human L-TGF- β 1 RGD_lasso3, L-TGF- β 1 RGE_lasso1, and Strep-His-GARP plasmids as in Fig. 1c.

Protein production

The secreted ectodomain of avb8 integrin was produced by transfecting ExpiCHO cells with integrin constructs following the previous protocol¹⁵. After 5 days of growth, cells were centrifuged, and the supernatant was filtered through a 0.2 μ m PES membrane (Millipore). Protein was purified from supernatant via affinity chromatography using a Protein G column crosslinked with the 8B8 antibody, which binds to α v integrin¹⁶. Elution was achieved with 100 mM glycine (pH 2.5), followed by buffer adjustment

and size exclusion chromatography (Superose 6 Increase 10/300 GL, GE Healthcare) in 20 mM Tris-HCl pH 7.4, 150 mM NaCl, 1 mM CaCl₂ and 1 mM MgCl₂.

To produce secreted mutant L-TGF-b1/GARP, Expi293 cells were transiently transfected with three 3 plasmids: L-TGF- b1_R249A_RGE_lasso1, L-TGF- b1_R249A_RGD_lasso3, and GARP ectodomain tagged with a Strep-His tag. The supernatant was collected by centrifuging the cell culture which grew for 5 days and then filtered through a 0.2 µm PES membrane. Protein purification was done using Ni-NTA agarose, followed by washing with a buffer containing 0.6 M NaCl, 0.01 M Tris (pH 8.0), and elution with 250 mM imidazole in TBS. The eluted protein was applied to a Strep-tactin agarose column and washed with TBS. To remove the tag, HRV-3C protease was added, and the mixture was incubated overnight at 4°C. Finally, the protein was concentrated to about 1 mg/ml in a TBS buffer using centrifugal concentrators.

Mutant L-TGF-b1/GARP and avb8 was first incubated at room temperature for 30 min, subjected to size exclusion chromatography and, correct peaks were pooled and concentrated to 0.31 mg/ml.

28G11 (Biolegend, San Diego, CA) was used without further purification.

Cryo-EM

Purified mutant avb8/L-TGF-b1/GARP were incubated with 28G11 (1 mg/ml) at room temperature for 30 min at a molar ratio of 1:1, the final protein complex concentration is 0.37 mg/ml. For cryo-EM grid preparation, 3 µl of the complex was deposited onto Quantifoil 100 holey carbon films Au 300 mesh R 1.2/1/3, grids were glow-discharged for 30 s at 15 mA prior to sample application and freezing. The complexes were frozen using a FEI Vitrobot Mark IV using a 1 s blot time. All grids were frozen with 100% humidity at 22 °C and plunge-frozen in liquid ethane cooled by liquid nitrogen.

The data set was collected on a Thermo Fisher 200 KeV Glacios equipped with a GATAN K3 direct detector camera. 1,324 movies were collected at a nominal magnification of 69,000x, the defocus range was set to be between - 1.1 and - 2.2 µm. The detector pixel size was 0.576 Å and the dose was 63 e⁻/Å².

The data processing of avb8/L-TGF-b1/GARP/28G11 was carried out with CryoSPARC, with workflow shown in Extended Data Fig. 1c. The nominal resolution is estimated from gold standard FSC = 0.143 criterion. Final reconstruction and directional FSC (cFSCs in CryoSPARC) show clear sign of anisotropic resolution, indicating that the dataset suffers preferred orientation. Docking of atomic model of avb8/L-TGF-b1/GARP and a generic Fab into the density map were performed using UCSF Chimera¹⁷. The location of 28G11 on L-TGF-b1 matches the previous cryo-EM structure of L-TGF-b1/GARP/28G11¹¹.

X-ray map density calculation

The structure factor of L-TGF-b1 (PDB: 3RJR) was obtained from PDB, and converted to mrc file which can be recognized by UCSF Chimera in COOT.

AlphaFold prediction

The predictions of human L-TGF-b1 dimers, was performed using two same TGF-b chains without signal peptide or templates by AlphaFold

(<https://colab.research.google.com/github/deepmind/alphafold/blob/main/notebooks/AlphaFold.ipynb>)¹⁸.

Sequence alignments

Multiple protein sequence alignments for L-TGF-b were generated using Clustal Omega [<https://academic.oup.com/nar/article/47/W1/W636/5446251>].

Antibody binding assay

ELISA plates were coated with serial dilutions of recombinant TGF-b1/GARP or recombinant TGF-b1_lasso3/GARP (10 µg/ml) in PBS for 1 hr at RT. Wells were then washed in PBS and blocked (5% BSA) in PBS for 1 hour at RT. 28G11 or isotype control antibody were added (1 µg/ml) in PBS for 1 hr at RT. After washing in PBS tween-20 (0.05%), bound antibodies were detected using anti-mouse-HRP using TMB substrate and colorimetric detection (Glomax Explorer, Promega).

Declarations

DECLARATION OF INTERESTS

S.L.N. is on the scientific advisory board (SAB) of Corbus Pharmaceuticals, LLC. Y.C. is on the SABs of ShuiMu BioSciences Ltd. and Pamplona Therapeutics.

Acknowledgements:

Equipment at the UCSF cryo-EM facility was supported by NIH grants S100D020054, S100D021741, and S100D025881 and is managed by D. Bulkley and G. Gilbert. We thank M. Harrington and J. Li for computational support. This work was partially supported by NIH R01HL134183 and R01HL165175 (S.L.N. and Y.C.). Y.C. is an investigator of the Howard Hughes Medical Institute. BioRender was used for some figure preparations.

Data availability

Cryo-EM map of mutant avb8/L-TGF-b/GARP/28G11 is deposited to EMDB with accession number EMDB-xxxxx.

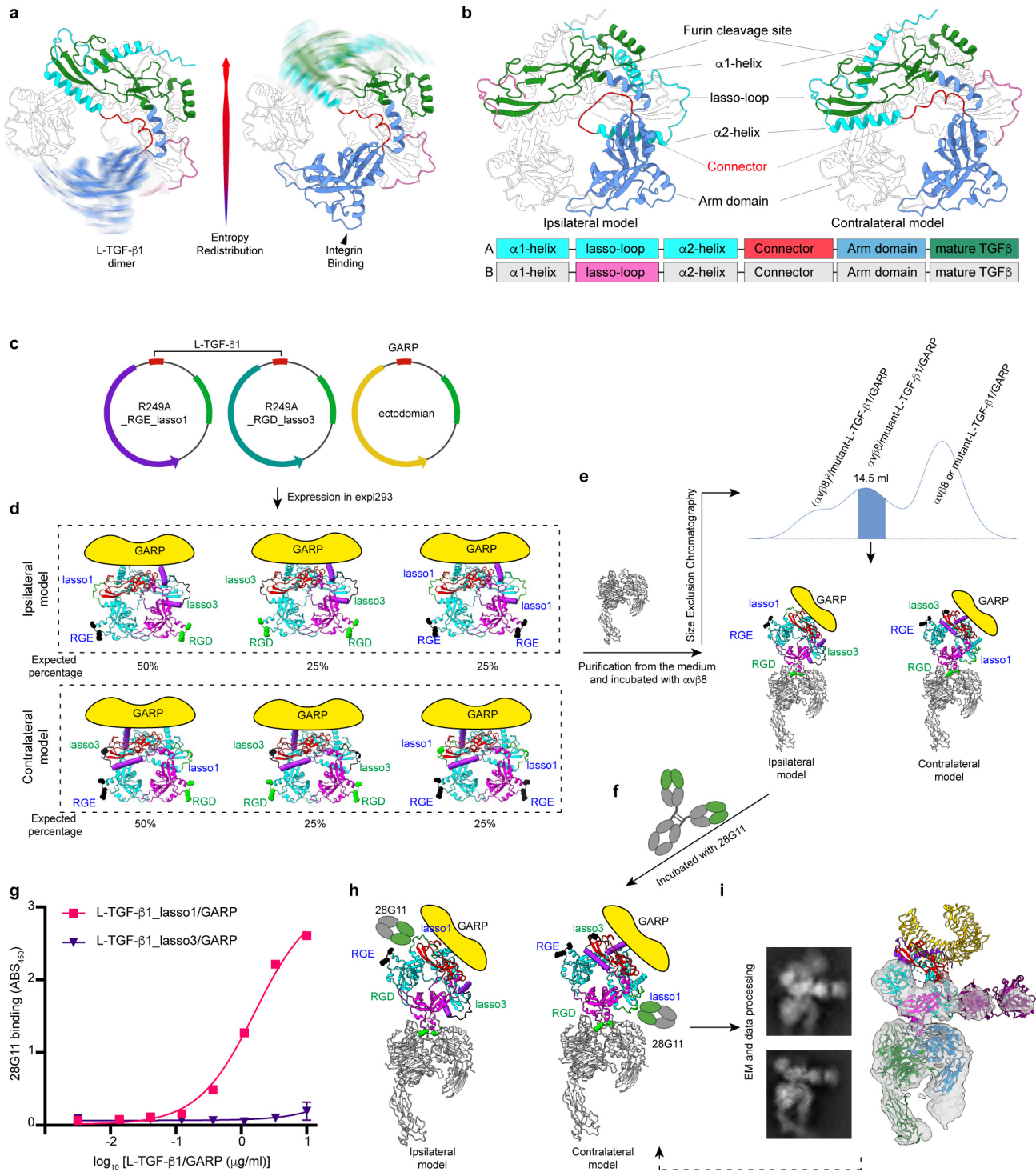
References

1. Akhurst, R.J. (2017). Targeting TGF-beta Signaling for Therapeutic Gain. *Cold Spring Harb Perspect Biol* 9. 10.1101/cshperspect.a022301.
2. Mu, D., Cambier, S., Fjellbirkeland, L., Baron, J.L., Munger, J.S., Kawakatsu, H., Sheppard, D., Broaddus, V.C., and Nishimura, S.L. (2002). The integrin alpha(v)beta8 mediates epithelial homeostasis through MT1-MMP-dependent activation of TGF-beta1. *J Cell Biol* 157, 493-507. 10.1083/jcb.200109100.
3. Munger, J.S., Huang, X., Kawakatsu, H., Griffiths, M.J., Dalton, S.L., Wu, J., Pittet, J.F., Kaminski, N., Garat, C., Matthay, M.A., et al. (1999). The integrin alpha v beta 6 binds and activates latent TGF beta 1: a mechanism for regulating pulmonary inflammation and fibrosis. *Cell* 96, 319-328.
4. Annes, J.P., Munger, J.S., and Rifkin, D.B. (2003). Making sense of latent TGFbeta activation. *J Cell Sci* 116, 217-224.
5. Shi, M., Zhu, J., Wang, R., Chen, X., Mi, L., Walz, T., and Springer, T.A. (2011). Latent TGF-beta structure and activation. *Nature* 474, 343-349. 10.1038/nature10152.
6. Lienart, S., Merceron, R., Vanderaa, C., Lambert, F., Colau, D., Stockis, J., van der Woning, B., De Haard, H., Saunders, M., Coulie, P.G., et al. (2018). Structural basis of latent TGF-beta1 presentation and activation by GARP on human regulatory T cells. *Science* 362, 952-956. 10.1126/science.aau2909.
7. Jin, M., Seed, R.I., Cai, G., Shing, T., Wang, L., Ito, S., Cormier, A., Wankowicz, S.A., Jespersen, J.M., Baron, J.L., et al. (2024). Dynamic allostery drives autocrine and paracrine TGF-beta signaling. *Cell*. 10.1016/j.cell.2024.08.036.
8. Dong, X., Zhao, B., Iacob, R.E., Zhu, J., Koksai, A.C., Lu, C., Engen, J.R., and Springer, T.A. (2017). Force interacts with macromolecular structure in activation of TGF-beta. *Nature* 542, 55-59. 10.1038/nature21035.
9. Duan, Z., Lin, X., Wang, L., Zhen, Q., Jiang, Y., Chen, C., Yang, J., Lee, C.H., Qin, Y., Li, Y., et al. (2022). Specificity of TGF-β1 signal designated by LRRC33 and integrin α. *Nat Commun* 13, 4988. 10.1038/s41467-022-32655-9.
10. Zhao, B., Xu, S., Dong, X., Lu, C., and Springer, T.A. (2018). Prodomain-growth factor swapping in the structure of pro-TGF-β1. *J Biol Chem* 293, 1579-1589. 10.1074/jbc.M117.809657.
11. Igney, F.H., Ebenhoch, R., Schiele, F., and Nar, H. (2023). Anti-GARP Antibodies Inhibit Release of TGF-β by Regulatory T Cells via Different Modes of Action, but Do Not Influence Their Function In Vitro. *Immunohorizons* 7, 200-212. 10.4049/immunohorizons.2200072.
12. Wang, X., Fischer, G., and Hyvönen, M. (2016). Structure and activation of pro-activin A. *Nat Commun* 7, 12052. 10.1038/ncomms12052.
13. Cotton, T.R., Fischer, G., Wang, X., McCoy, J.C., Czepnik, M., Thompson, T.B., and Hyvönen, M. (2018). Structure of the human myostatin precursor and determinants of growth factor latency. *EMBO J* 37, 367-383. 10.15252/emboj.201797883.
14. Le, V.Q., Iacob, R.E., Zhao, B., Su, Y., Tian, Y., Toohey, C., Engen, J.R., and Springer, T.A. (2022). Protection of the Prodomain α1-Helix Correlates with Latency in the Transforming Growth Factor-β Family. *J Mol Biol* 434, 167439. 10.1016/j.jmb.2021.167439.
15. Campbell, M.G., Cormier, A., Ito, S., Seed, R.I., Bondesson, A.J., Lou, J., Marks, J.D., Baron, J.L., Cheng, Y., and Nishimura, S.L. (2020). Cryo-EM Reveals Integrin-Mediated TGF-β Activation without Release

from Latent TGF- β . *Cell* 180, 490-501.e416. 10.1016/j.cell.2019.12.030.

16. Weinacker, A., Chen, A., Agrez, M., Cone, R.I., Nishimura, S., Wayner, E., Pytela, R., and Sheppard, D. (1994). Role of the integrin alpha v beta 6 in cell attachment to fibronectin. Heterologous expression of intact and secreted forms of the receptor. *J Biol Chem* 269, 6940-6948.
17. Pettersen, E.F., Goddard, T.D., Huang, C.C., Couch, G.S., Greenblatt, D.M., Meng, E.C., and Ferrin, T.E. (2004). UCSF Chimera--a visualization system for exploratory research and analysis. *J Comput Chem* 25, 1605-1612. 10.1002/jcc.20084.
18. Jumper, J., Evans, R., Pritzel, A., Green, T., Figurnov, M., Ronneberger, O., Tunyasuvunakool, K., Bates, R., Zidek, A., Potapenko, A., et al. (2021). Highly accurate protein structure prediction with AlphaFold. *Nature* 596, 583-589. 10.1038/s41586-021-03819-2.

Figures



Jin et al. Fig. 1

Figure 1

Experiment design and determination of domain architecture of L-TGF-b1/GARP

a, Ribbon diagram illustrating redistribution of conformational entropy in L-TGF-b1 from the RGD site to contralateral lasso loop prior (left) and after (right) avb8 binding⁷. **b**, Ribbon diagram illustrating two possible architectures of L-TGF-b1 dimer, in which the straitjacket domain of each prodomain is connected

ipsilaterally (left) or contralaterally (right) with the arm domain. Color scheme in ribbon diagram and domain arrangements are the same. **c**, Plasmid constructs of L-TGF-b1_R249A_RGE_lasso1 (left), L-TGF-b1_R249A_RGD_lasso3 (middle) and GARP (right). **d**, Anticipated expression products and their proportions from the 1:1:1 transfection of Expi293 cells. Ribbon diagrams of L-TGF-b1 in ipsilateral (upper) or contralateral (bottom) architectures are predicted by AlphaFold. **e**, SEC profile (middle) of purified mutant L-TGF-b1/GARP incubated with avb8 ectodomain (left). The shaded peak contains two possible complexes (bottom). **f**, Incubation of monoclonal antibody clone 28G11 with the SEC purified complex. **g**, ELISA confirms that 28G11 only binds lasso1 but not lasso3. Shown is a single experiment with error bars showing SD from 2 experimental replicates. **h**, Two models illustrating binding of 28G11 to mutant L-TGF-b1/GARP in ipsilateral (left) and contralateral (right) architectures. **i**, Representative 2D class averages and 3D reconstruction with atomic models of a generic Fab and contralateral L-TGF-b1/GARP docked.

Supplementary Files

This is a list of supplementary files associated with this preprint. Click to download.

- [FigS1.jpg](#)